Dust devil tracks and wind streaks in the North Polar Region of Mars: A study of the 2007 Phoenix Mars Lander Sites

Nathan B. Drake,[1] Leslie K. Tamppari,[2] R. David Baker,[1] Bruce A. Cantor,[3] and Amy S. Hale[2]

Received 10 March 2006; revised 10 July 2006; accepted 31 July 2006; published 8 September 2006.

[1] The 65–72 latitude band of the North Polar Region of Mars, where the 2007 Phoenix Mars Lander will land, was studied using satellite images from the Mars Global Surveyor (MGS) Mars Orbiter Camera Narrow-Angle (MOC-NA) camera. Dust devil tracks (DDT) and wind streaks (WS) were observed and recorded as surface evidence for winds. No active dust devils (DDs) were observed. 162 MOC-NA images, 10.3% of total images, contained DDT/WS. Phoenix landing Region C (295–315W) had the highest concentration of images containing DDT/WS per number of available images (20.9%); Region D (130–150W) had the lowest (3.5%). DDT and WS direction were recorded for Phoenix landing regions A (110–130W), B (240–260W), and C to infer local wind direction. Region A showed dominant northwest-southeast DDT/WS, Region B showed dominant north-south, east-west and northeast-southwest DDT/WS, and region C showed dominant west/northwest – east/southeast DDT/WS. Results indicate the 2007 Phoenix Lander has the highest probability of landing near DDT/WS in landing Region C. Based on DDT/WS linearity, we infer Phoenix would likely encounter directionally consistent background wind in any of the three regions. **Citation:** Drake, N. B., L. K. Tamppari, R. D. Baker, B. A. Cantor, and A. S. Hale (2006), Dust devil tracks and wind streaks in the North Polar Region of Mars: A study of the 2007 Phoenix Mars Lander Sites, *Geophys. Res. Lett.*, *33*, L19S02, doi:10.1029/2006GL026270.

1. Introduction

1.1. Dust Devils (DDs), Dust Devil Tracks (DDT), and Wind Streaks (WS)

[2] Martian DDs are convective vortices that loft dust into the atmosphere through vortical winds, saltation, and pressure variations near the vortex center [*Greeley and Iversen*, 1985; *Greeley et al.*, 2003]. DD activity is observed to peak in late morning to early afternoon Martian time [*Murphy and Nelli*, 2002] and DDs are believed to help maintain the observed 'background' dust load in the Martian atmosphere [*Basu et al.*, 2004; *Fisher et al.*, 2005; B. A. Cantor et al., MOC observations of Martian dust devils and their tracks (September 1997–January 2006) and evaluation of theoretical vortex models, September 1997–January 2006, submitted to *Journal of Geophysical Research*, 2006, hereinafter referred to as Cantor et al., submitted manuscript, 2006]. Martian DDs as large as 1 km in diameter and several kilometers high were first recorded in Viking Orbiter images [*Thomas and Gierasch*, 1985] and both active DDs and DDT have been extensively recorded in images from the Mars Global Surveyor Narrow-Angle Mars Orbiter Camera (MGS MOC-NA) [*Cantor et al.*, 2002, also submitted manuscript, 2006; *Balme et al.*, 2003; *Fisher et al.*, 2005]. DDT and WS are seen at nearly all latitudes and elevations on the Martian surface [*Malin and Edgett*, 2001; *Balme et al.*, 2003; *Fisher et al.*, 2005] but no active DDs poleward of 63N have been observed at 1400 LST (the approximate time at which MGS captures images) (Cantor et al., submitted manuscript, 2006). The MOC-NA system can provide images at a resolution of 0.5 m pixel^{-1}, with an average of 3–6 m pixel^{-1}, and has observed the Polar Regions of Mars in detail [*Malin and Edgett*, 2001]. Observable DDT and WS in MOC-NA images are typically several meters to several kilometers in width [*Balme et al.*, 2003; *Fisher et al.*, 2005].

[3] DDs can remove thin layers of dust as they traverse the Martian ground, exposing the regolith beneath to create DDT that are lighter or darker than the surrounding terrain [*Edgett and Malin*, 2000; *Greeley et al.*, 2004; Cantor et al., submitted manuscript, 2006]. Non-vortical surface winds are also capable of removing surface material, resulting in surface albedo changes called WS [*Christensen*, 1988; Cantor et al., submitted manuscript, 2006]. These wind-induced albedo features [*Veverka*, 1976] tend to form as linear streaks near or in the lee of topographic relief and are morphologically different from DDT (Cantor et al., submitted manuscript, 2006). Examples of both DDT and WS in the Phoenix latitude band are shown in Figures 1a–1c. Because there is sometimes ambiguity in distinguishing between DDT and WS, we characterize both as well-defined streaks superposed on the Martian surface and do not distinguish them in quantitative analysis. In addition, we are interested in overall wind directions and both DDs and WS are thought to serve as "wind vanes", indicating the direction of local wind at the time of formation [*Greeley et al.*, 2005].

1.2. Phoenix Mars Lander

[4] There have been four 20-degree landing locations in the 65–72N latitude band considered for the 2007 Phoenix Mars Lander: Region A (110–130W), B (240–260W), C (295–315W) and D (130–150W). The Phoenix upward-looking LIDAR (light detection and ranging), surface stereo imager, and pressure sensor all have the ability to detect DDs. Mars Pathfinder recorded DDs as short-term variations in measured surface pressure, wind velocity, and air

[1]Department of Physics, Austin College, Sherman, Texas, USA.
[2]Jet Propulsion Laboratory, California Institute of Technology, Pasadena, California, USA.
[3]Malin Space Science Systems, San Diego, California, USA.

0094-8276/06/2006GL026270$05.00

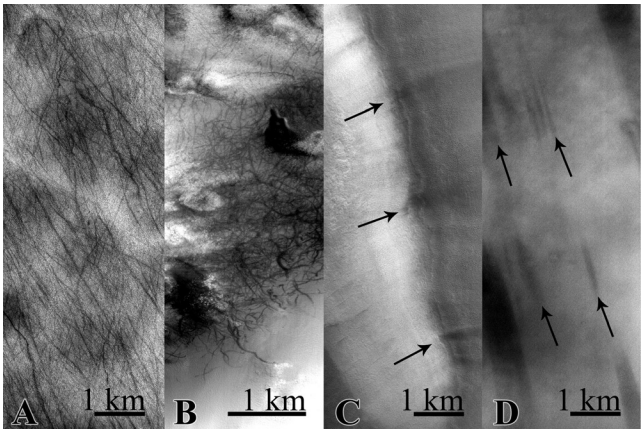

Figure 1. MOC-NA Images: (a) M22-01024 (67.57N, 57.87W) Many linear and parallel dust devil tracks are seen over spotted albedo patterns. This image is representative of the majority of observed images containing dust devil tracks. (b) M00-01253 (65.4N, 182.48W) Less typical curvilinear and nonparallel dust devils tracks are seen, indicating light winds. (c) M19-00708 (64.74N, 162.99W) Wind streaks are observed as wind flows over a Martian ridge. (d) E05-03579 (65.29N, 297.03W) Low-albedo surface features may be obscured by increased optical depth and shadows cast from atmospheric dust and condensate clouds. Images such as this were not included in the final dust devil track and wind streak count [*Malin et al.*, 2006].

temperature [*Schofield and Barnes*, 1997], indicating the Phoenix atmospheric instrument suite will be adequately equipped to detect and image passing DDs. To help the Phoenix Lander team better understand aeolian processes in the Phoenix landing regions, this study was designed to: (1) search the 65–72N latitude band for the presence of DDs, DDT, and WS using MOC-NA images, because this had never been done before; (2) collect statistics regarding the number, location, and direction of these phenomena; and (3) provide an estimate of the predominant local wind direction in each Phoenix Landing Region.

2. MOC-NA Image Analysis

[5] All 1,734 MOC-NA images in the 65–72N latitude band of Mars were acquired from Malin Space Science Systems MOC Database. These images spanned the life of MGS, from its initial aerobraking phase (AB) beginning 15 September 1997 (where the elliptical orbit of the spacecraft yielded variability in the local time of observations), to science phase four (S04) (where the orbit of MGS had stabilized to capture images of Mars at roughly 1400 LST) ending 31 March 2005. Images were examined for the presence of DDs, DDT and WS. Corrupt or oversaturated images were discarded. Some images contained shadows cast from atmospheric dust and condensate clouds that may have obscured DDT and WS on the surface. These "atmospherically obscured" images were not included in the total DDT and WS count.

[6] A database was created to record images containing DDs, DDT, WS, and other unique terrain and atmospheric features. Latitude and longitude of image center, resolution, image name, and areocentric longitude of the sun (L_s) were recorded for every image. The database summary provides the number of images containing DDT and WS in each landing region, as well as the total number of images in each region.

[7] Map-projected MOC-NA images in Phoenix landing Regions A, B, and C containing DDT/WS were studied to determine track/streak direction. Region D was not considered because the project team has descoped it at this time. The direction of DDT and WS was recorded by taking an average of five linear measurements along different lengths of the DDT/WS. These data were plotted in histogram fashion based on frequency of DDT/WS orientation within 10° bins for each landing region. The DDT and WS direction data provides an estimate of the wind direction, with the caveat that wind direction could be oriented in one of two directions (e.g., a north-south DDT/WS could indicate either northerly or southerly wind).

3. Results of MOC-NA Image Survey of 65–72N Phoenix Latitude Band

[8] Of the 1,734 available MOC-NA images, only 1,558 were of usable quality. Available images were evenly distributed across the 65–72N latitude band within ±0.4 degrees of the latitude-band center based on the average latitudinal coordinates of the center of all available MOC-NA images. A total of 162 images (10.3% of the total available) contained DDT or WS (Figures 2 and 3). No active DDs were observed in any MOC-NA image. The combined set of DDT and WS that could be seen to initiate and terminate within MOC-NA images exhibited lengths from ~50 m to over 16 km, with the longest DDT/WS usually extending across smooth, flat terrain. Length could not be determined for approximately 75% of all observed DDT and WS because they extended outside MOC-NA images. Because there were no pairs of overlapping MOC-NA images which contained DDT or WS in this region,

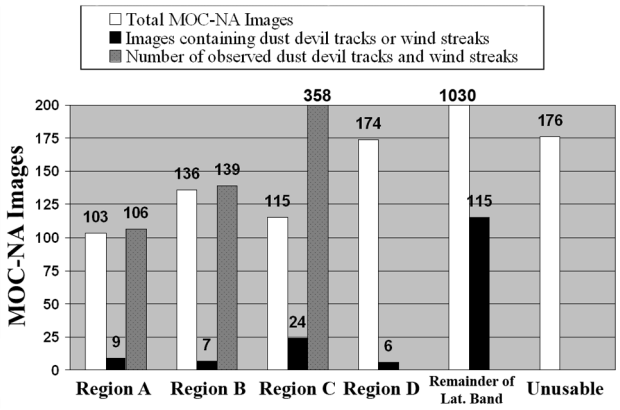

Figure 2. Statistics of MOC-NA images used in this study. Region C contained the highest number of images containing dust devil tracks and wind streaks, as well as the highest total number of tracks/streaks in the three surveyed landing regions. Region D was not analyzed for number of dust devil tracks and wind streaks because it is no longer a possible Phoenix landing site.

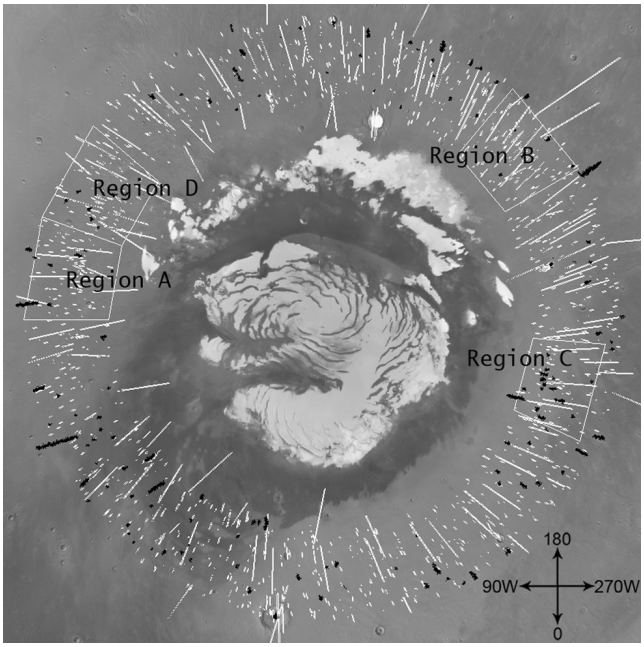

Figure 3. Map of the Phoenix Latitude Band (65–72) in the North Polar Region of Mars. Landing Regions A (250–270E), B (120–140E), C (65–85E), and D (230–250E) are shown. White lines indicate the location of MOC-NA images included in this study, black lines are MOC-NA images containing dust devil tracks or wind streaks.

seasonal variance of DDT and WS could not be determined. Many DDT were observed in regions with contrasting surface albedo (Figure 1).

[9] Phoenix landing Region C had the highest percentage of images containing DDT and WS per number of available images (20.9%), nearly double the amount found in the rest of the latitude band. Region C also contained the greatest total number of DDT and WS (358) and had the highest ratio of DDT/WS per number of regional images (Figure 2). DDT and WS direction were calculated for Phoenix landing Region A, B, and C. Because direction of flow was unknown, all DDT/WS were assumed to be oriented between 0° and 180°, then extended from 180° to 360° because flow direction may be antiparallel to the recorded value. Region A showed dominant NW-SE DDT/WS alignment, region B showed N-S, E-W and NE-SW orientation, and region C showed dominant WNW-ESE orientation (Figure 4).

4. Discussion

[10] This is the first study documenting DDT and WS in the North Polar Region (65–72N) of Mars. A large number of the total images (10.3%) contained DDT or WS, indicating the 65–72N latitude band has the necessary regolith particle size and albedo conditions for DDT and WS to appear. *Greeley et al.* [1992] suggest that high-albedo surfaces may be deposits of fine particle (dust) deposition, while low-albedo surfaces may consist of coarser, darker particles. These surfaces may have been swept free of fine dust, exposing a darker underlying substrate. This theory has been experimentally verified by *Greeley et al.* [2004]. Many of the MOC-NA images containing DDT and WS in this study were characterized by spotted albedo patterns, possibly indicating that a fine light dust overlays a darker substrate in these regions (Figure 1), allowing DDs and WS to create visible tracks/streaks more easily.

[11] The precise cause of DD formation in the North Polar Region of Mars remains uncertain. DDT in this study were often observed around and within topographic features. These observations suggest that topographic features may help generate vorticity that develops into DDs [e.g., *Renno et al.*, 2004]. A recent DD model [*Toigo et al.*, 2003] found that the planetary boundary layer (for equatorial conditions) may rapidly develop horizontal vorticity as a result of free convection, even in the absence of background wind. The observed spotted albedo terrain in MOC-NA images we examined may give rise to uneven heat convection across the planetary boundary layer, generating DDs even with no background wind present.

[12] It is unlikely, however, that DDT and WS in this study formed in the absence of background wind. Because DDT and WS are pushed by local winds, they are thought to serve as "wind vanes" [*Greeley et al.*, 2005], indicating the

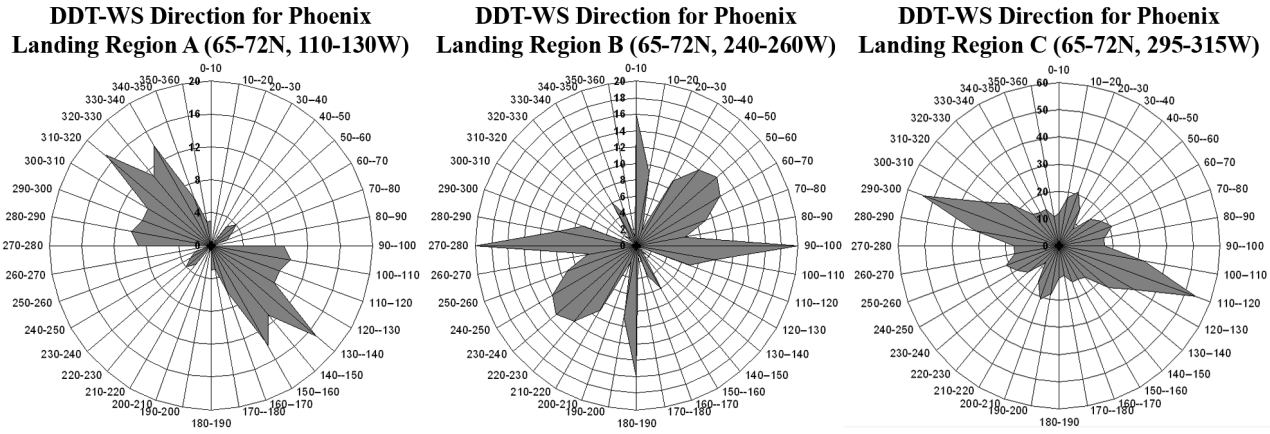

Figure 4. Dust devil track and wind streak direction in Phoenix landing regions A, B, and C. Dust devil tracks and wind streaks are believed to be pushed by local winds [*Greeley et al.*, 2005], making it possible to infer local wind direction. Inferred wind direction may be parallel or antiparallel to track/streak orientation.

prevailing wind directions at the time of formation. The linearity of observed DDT and WS in these regions suggest the presence of local wind at the time of formation (Figure 1) [*Greeley et al.*, 2005]. Model simulations show that DDs can form in the presence of strong winds [*Toigo et al.*, 2003]. Recent analysis of other MOC images suggests that DDs are most often formed in light winds or at the leading edge of cold fronts of dust storms (Cantor et al., submitted manuscript, 2006).

[13] Region C contained the greatest total number of DDT and WS (358) and the highest ratio of DDT and WS per number of images (Figure 2), indicating the Phoenix Landing Region C is either the most active region of those examined or retains the signature of these events over the longest time period. DDT and WS directions appear to be narrowly aligned in a NW-SE direction in Regions A and C, but have a broader distribution in Region B (Figure 4).

[14] No active DDs were observed. There are three possible explanations for the lack of active DDs: 1) there is not enough MOC-NA spatial nor temporal coverage of this region to capture active DDs, 2) lofted dust particles in an active DD in this region may be too fine or not of sufficient optical depth to produce sufficient contrast to be visible, 3) DDs do not peak in activity in local afternoon in this region; they are active during other parts of the day (only ~12% of observed DDs at the Pathfinder site occurred during 1400–1500 LST, the time when MGS captures images [*Murphy and Nelli*, 2002]).

[15] Additional images and in situ data of the Phoenix latitude zone will lend insight into dust devil formation, potential DD seasonal variability, and flow direction at this latitude. The Phoenix lander will measure atmospheric optical depth, near-surface pressure, amount and distribution of scatterers overhead, and surface regolith properties of the North Polar Region during the Martian northern summer. The results presented here indicate that a landing location for Phoenix in Region C will maximize the chances of observing active aeolian processes, although Regions A and B may also provide this opportunity.

[16] **Acknowledgments.** We thank the California Institute of Technology's Student Undergraduate Research Fellowship and the Lilly Foundation at Austin College for support of this work. Part of the research described in this paper was carried out at the Jet Propulsion Laboratory, California Institute of Technology, under a contract with the National Aeronautics and Space Administration.

References

Balme, M., P. Whelley, and R. Greeley (2003), Mars: Dust devil track survey in Argyre Planitia and Hellas Basin, *J. Geophys. Res.*, *108*(E8), 5086, doi:10.1029/2003JE002096.

Basu, S., M. I. Richardson, and R. J. Wilson (2004), Simulation of the Martian dust cycle with the GFDL Mars GCM, *J. Geophys. Res.*, *108*(E8), E11006, doi:10.1029/2004JE002243.

Cantor, B., M. Malin, and K. Edgett (2002), Multiyear Mars Orbiter Camera (MOC) observations of repeated Martian weather phenomena during the northern summer season, *J. Geophys. Res.*, *107*(E3), 5014, doi:10.1029/2001JE001588.

Christensen, P. R. (1988), Global albedo variations of mars: Implications for active aeolian transport, deposition, and erosion, *J. Geophys. Res.*, *93*, 7611–7624.

Edgett, K. S., and M. C. Malin (2000), Martian dust raising and surface albedo controls: Thin, dark (and sometimes bright) streaks and dust devils in MGS high-resolution images, *Lunar Planet. Sci.* [CD-ROM], *XXXIII*, abstract 1073.

Fisher, J., M. Richardson, C. Newman, M. Szwast, C. Graf, S. Basu, S. Ewald, A. Toigo, and R. Wilson (2005), A survey of Martian dust devil activity using Mars Global Surveyor Mars Orbiter Camera images, *J. Geophys. Res.*, *110*, E03004, doi:10.1029/2003JE002165.

Greeley, R., and J. D. Iversen (1985), *Wind as Geologic Process on Earth, Mars, Venus, and Titan*, 333 pp, Cambridge Univ. Press, New York.

Greeley, R., N. Lancaster, S. Lee, and P. Thomas (1992), Martian aeolian processes, sediments and features, in *Mars*, edited by B. M. Jakowsky et al., pp. 730–776, Univ. of Ariz. Press, Tuscon.

Greeley, R., M. R. Balme, J. D. Iversen, S. Metzger, R. Mickelson, J. Phoreman, and B. White (2003), Martian dust devils: Laboratory simulations of particle threshold, *J. Geophys. Res.*, *108*(E5), 5041, doi:10.1029/2002JE001987.

Greeley, R., P. Whelley, and L. Neakrase (2004), Martian dust devils: Directions of movement inferred from their tracks, *Geophys. Res. Lett.*, *31*, L24702, doi:10.1029/2004GL021599.

Greeley, R., et al. (2005), Martian variable features: New insight from the Mars Express Orbiter and the Mars Exploration Rover Spirit, *J. Geophys. Res.*, *110*, E06002, doi:10.1029/2005JE002403.

Malin, M. C., and K. S. Edgett (2001), Mars Global Surveyor Mars Orbiter Camera: Interplanetary cruise through primary mission, *J. Geophys. Res.*, *106*(E10), 23,429–23,570.

Malin, M. C., K. S. Edgett, S. D. Davis, M. A. Caplinger, E. Jensen, K. D. Supulver, J. Sandoval, L. Posiolova, and R. Zimdar (2006), [M00-01253,M01-01267, M19-00708, E01-01654, E05-03579], Malin Space Science Systems Mars Orbiter Camera Image Gallery, San Diego, Calif. (Available at http://www.msss.com/mars_images/moc/)

Murphy, J., and S. Nelli (2002), Mars Pathfinder convective vortices: Frequency of occurrence, *Geophys. Res. Lett.*, *29*(23), 2103, doi:10.1029/2002GL015214.

Renno, N. O., et al. (2004), MATADOR 2002: A pilot field experiment on convective plumes and dust devils, *J. Geophys. Res.*, *109*, E07001, doi:10.1029/2003JE002219.

Schofield, J. T., and J. R. Barnes (1997), The Mars Pathfinder Atmospheric Structure Investigation/Meteorology (ASI/MET) experiment, *Science*, *278*, 1752–1758.

Thomas, P., and P. Gierasch (1985), Dust devils on Mars, *Science*, *230*, 170–175.

Toigo, A., M. Richardson, S. Ewald, and P. Gierasch (2003), Numerical simulation of Martian dust devils, *J. Geophys. Res.*, *108*(E6), 5047, doi:10.1029/2002JE002002.

Veverka, J. (1976), Variable features on Mars. VII—Dark filamentary markings on Mars, *Icarus*, *27*, 495–502.

R. D. Baker and N. B. Drake, Department of Physics, Austin College, Sherman, TX 75090, USA. (nathan.drake@gmail.com)

B. A. Cantor, Malin Space Science Systems, San Diego, CA 92191-0148, USA.

A. S. Hale and L. K. Tamppari, Jet Propulsion Laboratory, California Institute of Technology, Pasadena, CA 91109, USA.